Eye (2009) 23, 1845–1850

www.nature.com/eye

LABORATORY STUDY

Postsurgery corneal asphericity and spherical aberration due to ablation efficiency reduction and corneal remodelling in refractive surgeries

Y Kwon and S Bott

Abstract

Purpose **To explain the origin of changes in corneal asphericity and induced spherical aberration after laser refractive surgery.**
Methods **A rigorous model, CASIM (corneal ablation simulator), has been developed to model the ablation profile design, the shot-by-shot ablation process and the corneal remodelling that occurs through healing. The dependence of corneal asphericity, induced spherical aberration, and achieved refractive correction on corneal remodelling, and the ablation efficiency reduction caused by the angle of incidence of the excimer beam on the curved cornea are compared to the clinical outcomes reported in the literature.**
Results **When the exact Munnerlyn formula is used, the CASIM modelling and the clinical data exhibit a high degree of correlation. The modelling predicts that the postoperative cornea will be oblate, with substantial induced spherical aberration. A 6-month postsurgery asphericity is predicted by CASIM with a correlation of $R^2 = 0.94$. The corneal remodelling included in CASIM accounts, on the average, for 45 and 69% of the increase in asphericity and spherical aberration, respectively, with the remainder due to the ablation efficiency.**
Conclusions **The modelling shows that clinically observed increases in corneal asphericity and induction of spherical aberration can be explained by the effects of corneal remodelling due to healing and by the ablation efficiency reduction due to laser angle of incidence. The model is capable of predicting clinical outcomes for procedures performed with flying spot laser systems and could be used to design compensated ablation profiles to improve the clinical outcomes for custom as well as conventional laser refractive procedures.**

Eye (2009) **23,** 1845–1850; doi:10.1038/eye.2008.356; published online 5 December 2008

Keywords: refractive surgery; ablation efficiency; corneal asphericity; induced spherical aberration; clinical outcome

Introduction

In recent years, wavefront-guided customized laser refractive surgery has proven effective in improving patient visual performance. However, a better understanding of aberrations induced by the laser refractive surgery process could improve clinical outcomes. Clinical results show increased ocular aberrations,[1–5] particularly spherical aberration and coma, after refractive surgery. After myopic procedures, induced spherical aberrations tend to be positive and correlated with the magnitude of intended correction.[5–8] The increase in spherical aberration influences the visual function of the patient,[4,9] as measured by contrast-sensitivity function (CSF) and low luminance visual acuity. Further, if significant spherical aberration is induced by refractive surgery, the correction of defocus could also be affected.

Several studies report possible reasons for induced spherical aberrations. First, a change in corneal asphericity was reported by Holladay *et al*,[9,10] Mrochen and Seiler,[11] Hersh *et al*,[7] Anera

Alcon Laboratories Inc., Orlando, FL, USA

Correspondence: Y Kwon, Current position: Consultant at Omega Photonics, Oviedo, FL, USA
Tel: +407 462 9804;
Fax: +407 365 2994.
E-mail: young.kwon@colorado.edu

Received: 28 April 2008
Accepted in revised form: 28 October 2008
Published online: 5 December 2008

et al,[12] Jimenez *et al*,[13] and Gatinel *et al*.[14] They show that the postsurgery cornea becomes oblate; and could partly explain induced spherical aberration. However, it was unclear how ablation profiles based on the exact Munnerlyn formula could induce large changes in corneal asphericity, until Dorronsoro *et al*[15] developed an experimental correction factor, which could predict the increase in corneal asphericity in accordance with clinical data. Kwon *et al*[16] used a simulation model to explain the experimental data reported by Dorronsoro *et al*[15] and have shown that ablation efficiency reduction predicts ~90% of the increase for the type of laser used for those treatments. Second, corneal remodelling also contributes to the induction of high-order aberrations, as shown by Huang *et al*.[17] In addition, other factors, including ablation decentration, corneal biomechanical changes, and tracker performance may also contribute to the induction of high-order aberrations adding to the complexity of the prediction. A more precise understanding of the origins of induced spherical aberration could provide better surgical outcomes.

In this study, we use a rigorous simulation model for the entire surgical process, generating: an ablation profile from the measured wavefront errors, a shot pattern, the shot-by-shot ablation process, and remodelling of the cornea after surgery. The simulator, CASIM (corneal ablation simulator)[18] calculates the postoperative corneal topographic maps and vision metrics, including MTF, PSF-entropy, and visual strehl ratio, as well as the changes in corneal asphericity and induced spherical aberration.

Mrochen and Seiler[11] showed that the two factors—laser reflection losses at the cornea and non-normal incidence of the laser in the periphery—cause ablation efficiency reduction. Jimenez *et al*[19] proposed a correction formula that quantifies the effect of these two factors, based on the paraxial approximation, for the ablation depth $z_P(r)$:

$$z_P(r) = \frac{4Dr^2}{3} - \frac{D \cdot \mathrm{OZ}^2}{3} \tag{1}$$

where D is the attempted correction, OZ is the optical zone diameter, and r is the distance from the optical axis. An analytical expression was proposed for postsurgery asphericity to explain the notable increase in spherical aberration and change in corneal asphericity when the parabolic approximation of Munnerlyn formula is used. Jiménez *et al*[13] showed that pre- and postsurgery asphericity values scale with the cube of pre- to postcorneal radii. For an aspherical surface, spherical aberration is proportional to asphericity ($Q = p-1$),[8] which accounts for the increase in spherical aberration. However, when the exact Munnerlyn formula is used, without ablation efficiency reduction, Gatinel *et al*[14] reported that the postsurgery corneal asphericity does not increase. In exact Munnerlyn formula, $z_M(r)$ is given by:[20]

$$\begin{aligned} z_M(r) = &\sqrt{R^2 - r^2} - \sqrt{R'^2 - r^2} \\ &+ \sqrt{R'^2 - \mathrm{OZ}^2/4} - \sqrt{R^2 - \mathrm{OZ}^2/4} \end{aligned} \tag{2}$$

where r is the radial distance from the apex of the cornea. Dorronsoro *et al*[15] and Yoon *et al*[8] reported that the postsurgery corneal asphericity increases even when the Munnerlyn formula is used. Yoon *et al*[8] used the exact Munnerlyn formula with the ablation efficiency reduction model proposed by Mrochen and Seiler[11] to show increased asphericity and induced positive spherical aberration after myopic surgery. However, Yoon *et al*[8] found that the amount of increase in corneal asphericity and spherical aberration observed in the clinical data cannot be explained by the change of corneal shape alone. The major increase was accounted for by considering the biological response of cornea.

On the basis of the simulation results reported elsewhere,[16] corneal asphericity must increase, even when the exact Munnerlyn formula is used. The amount of increase largely depends on presurgery corneal asphericity and laser beam characteristics with the increase for different laser platforms in the range of 0.3–1.0 for 6 D corrections and 0.8–3.3 for 12 D corrections for typical presurgery asphericity values ($-0.3 < Q < 0$), without considering corneal remodelling. A natural question then arises: how much does the corneal remodelling contribute to the induction of spherical aberration? We compare the CASIM model results with the clinical data to answer this question. We compare individual postoperative patient asphericity values reported in the literature with predictions of our model, enabling us to (i) establish the extent to which our model can predict postsurgery corneal asphericity and induced spherical aberration, and (ii) ascertain whether alterations in corneal asphericity are due to the ablation efficiency reduction, or if other parameters/mechanisms are involved.

Materials and methods

Simulation model

With the flying spot laser system, the per-pulse ablation depth is given by Lambert–Beer's law:[21]

$$\begin{aligned} d &= \frac{1}{\alpha} \ln \frac{F_r}{F_{\mathrm{TH}}} \text{ if } F_r > F_{\mathrm{TH}} \\ &= 0 \text{ if } F_r \leqslant F_{\mathrm{TH}} \end{aligned} \tag{3}$$

where d is the ablation depth, α is the absorption

coefficient at the laser wavelength, F_r is the fluence at position r, and F_{TH} is the ablation threshold fluence. We used typical values of $\alpha = 2.9\,\mu m^{-1}$ and $F_{TH} = 60\,mJ/cm^2$.

The laser beam fluence, reflectance, and absorption vary with the position of laser pulse on the cornea due to corneal curvature. Accounting for these dependencies, the final expression for ablation depth equation becomes:[16]

$$d = \frac{1}{2\alpha_Z} \ln\left[\frac{F}{F_{TH}} \cos\Theta(1 - R_{REFL})\right] \quad (4)$$

where R_{REFL} is the reflectance at the beam position on the cornea and α_Z is the angle-dependent absorption coefficient. For the correction of myopia, the dioptric correction is related to the pre- and postoperative radii by:

$$D = 0.376\left(\frac{1}{R'} - \frac{1}{R}\right) \quad (5)$$

where R' and R are the radii of the curvature of the postsurgery and pr-surgery cornea, respectively. Using the Munnerlyn formula, we generate shot patterns for individual surgeries. Each shot removes a volume of tissue, volume per shot (VPS), found by:

$$VPS = \int_0^\infty d2\pi r dr \quad (6)$$

The number of shots required for a treatment depends on dioptric correction, optical zone, laser characteristics, and other parameters. For remodelling, we use the model proposed by Huang *et al*[17] with the remodelling parameter $s = 0.5$.

Clinical data

The data set (Table 1), provided by Jimenez and colleagues[22] included 24 eyes of 14 patients operated on using an ESIRIS scanning spot laser (SCHWIND, Germany). The corneal topography (curvature radius and p-factor) were measured with an EyeSys 2000 topographer following the Holladay Diagnostic Summary Report on corneal asphericity. We assumed a peak fluence of $400\,mJ/cm^2$ with a laser beam diameter of 0.9 mm.

Corneal asphericity and spherical aberration

Using CASIM, postsurgery cornea shape profiles were computed shot-by-shot based on the Munnerlyn formula. Corneal asphericity was calculated by CASIM by fitting the resulting corneal shapes to the conic function:

$$z = \frac{r^2/R_C}{1 + \sqrt{1 - (1+Q)(r^2/R_C^2)}} \quad (7)$$

where z is the height of the corneal surface, Q is the asphericity of the corneal surface, R_C is the radius of curvature of the cornea, and r is the distance from the apex of the cornea. We used a region of 4.5 mm diameter for the fitting, as the clinical data were obtained over this zone size, presurgery asphericity reported for individual eyes, and a presurgery apical corneal radius of 7.8 mm.

Spherical aberration is computed in CASIM as follows. After finding the axial best focus by tracing the ray through the postsurgery cornea, the optical path difference (OPD) through the cornea is calculated. A refractive index of $n = 1.376$ is used for a cornea. The OPD is fitted to up to an eighth-order Zernike polynomial. The resulting spherical coefficient is verified against the result obtained by a standard ray-tracing programme Zemax (Zemax Development Corp. WA, USA) using an aspheric corneal surface model.

Figure 1 shows the corneal asphericity and spherical aberration for three apical corneal radii as examples. For a myopic correction of 9 D, we obtain the postsurgery apical radius of $R_C = 9.59$ mm using Eq. (5). Another graph for $R_C = 9.35$ mm is drawn for the purpose of comparison, corresponding to a 1-D undercorrection.

Eye no. 24 had a presurgery asphericity of $Q = -0.16$ and a 6-month postsurgery asphericity of $Q = 0.99$ as indicated on the graph. For a given corneal shape, undercorrection causes more induced spherical aberration. However, for a given amount of induced spherical aberration, a smaller change in asphericity is obtained with undercorrection. Corneal remodelling changes the corneal shape in postsurgery eyes by making the centre of the cornea flatter and the periphery steeper, resulting in a more oblate cornea. This causes changes in the best-fit radius of curvature as well as the corneal asphericity. Therefore, the complex interaction between preoperative corneal shape and induced spherical aberration is best found using accurate, detailed models, such as CASIM. Also, by observing the point of intersection of the three graphs in Figure 1, the value of corneal asphericity corresponding to zero spherical aberration is found to be $Q = -0.53$.

Results

Figure 2 presents the correlation between postsurgery corneal asphericity (6 months) and simulated post-healed corneal asphericity for 24 eyes. The average clinical

Table 1 Corneal asphericity corresponding to the eyes operated on. Clinical data for presurgery and 6 months after LASIK are shown. The clinical data are provided by Jimenez and colleagues[22]

Cases (eye)	*D*	*Presurgery*	*6-month postsurgery*	*Computed before healing*	*Computed after healing*
1	−1.25	−0.14	+0.09	−0.08	+0.00
2	−1.5	−0.21	+0.02	−0.13	−0.05
3	−1.75	−0.21	−0.09	−0.11	−0.02
4	−2	+0.03	+0.37	+0.16	+0.26
5	−2.5	−0.25	+0.27	+0.02	+0.13
6	−2.75	−0.25	+0.16	−0.11	+0.04
7	−2.75	+0.03	+0.31	+0.23	+0.36
8	−3	−0.06	+0.36	+0.11	+0.27
9	−3.75	−0.17	+0.20	+0.03	+0.23
10	−3.75	−0.30	+0.01	−0.13	+0.07
11	−4	−0.29	+0.24	−0.14	+0.12
12	−4	−0.17	+0.22	+0.01	+0.26
13	−4.5	−0.30	+0.09	−0.04	+0.17
14	−5	−0.09	+0.54	+0.20	+0.47
15	−5.5	+0.16	+0.72	+0.63	+0.85
16	−6	−0.03	+0.76	+0.39	+0.66
17	−6	−0.10	+0.53	+0.29	+0.57
18	−6.5	+0.19	+1.04	+0.75	+1.01
19	−7	−0.18	+0.61	+0.25	+0.58
20	−7	−0.02	+0.62	+0.49	+0.80
21	−8	−0.03	+0.67	+0.55	+0.90
22	−8.5	−0.32	+0.37	+0.10	+0.53
23	−8.5	−0.10	+0.79	+0.47	+0.85
24	−9	−0.16	+0.99	+0.41	+0.82

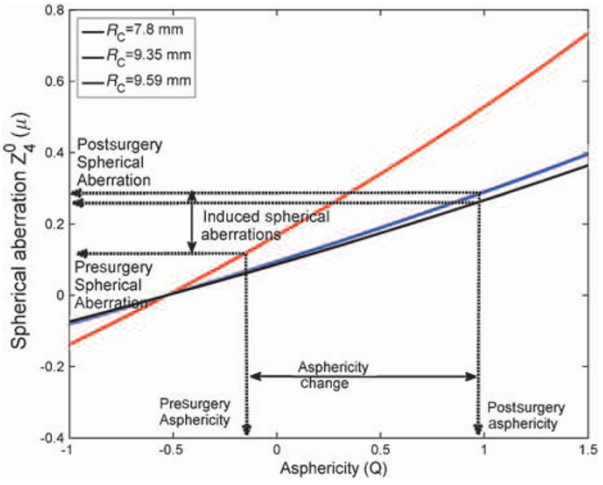

Figure 1 Calculated spherical aberration *vs* corneal asphericity. The optical zone size for Zernike fitting is 4.5 mm. From the data for eye no. 24, the presugery apshericity and 6-month postsurgery asphericity are used to show the relationship between asphericity change, and induced spherical aberrations. Also from the crossing of three graphs, the spherical aberration free cornea, corresponding to asphericity Q = −0.53 can be found.

asphericity before and after surgery was −0.12 and 0.41, respectively. The correlation between actual clinical and simulated asphericity, including corneal remodelling is $R^2 = 0.94$. Figure 3 shows postsurgery corneal asphericity before and after remodelling. The contribution of ablation efficiency reduction to the corneal asphericity, 0.30 on average, can be found from postsurgical simulated corneal profiles. The average contribution of ablation efficiency reduction and the remodelling process to the change of corneal asphericity are 55 and 45%, respectively.

Using the presurgery corneal asphericity and apical radius of the cornea, we can calculate the corneal contribution to spherical aberration for the preoperative eyes. By subtracting the presurgery spherical aberration from the postsurgery spherical aberration, we can estimate the induced spherical aberration before and after remodelling (Figure 4). The computed presurgery spherical aberration of a cornea with 4.5-mm pupil size is $0.11 \pm 0.04\,\mu$m. The computed spherical aberrations for the cornea, before and after remodelling, are $0.14 \pm 0.05\,\mu$m and $0.21 \pm 0.08\,\mu$m, respectively. The changes in spherical aberrations, that is, induced spherical aberrations before and after remodelling, are computed as 0.03 ± 0.02 and $0.09 \pm 0.05\,\mu$m. The average contribution of ablation efficiency reduction and the remodelling process to the change of spherical aberration are 31 and 69%, respectively.

Discussion

We have modelled the increase in postsurgery corneal asphericities for 24 eyes reported by Anera *et al*[22] using

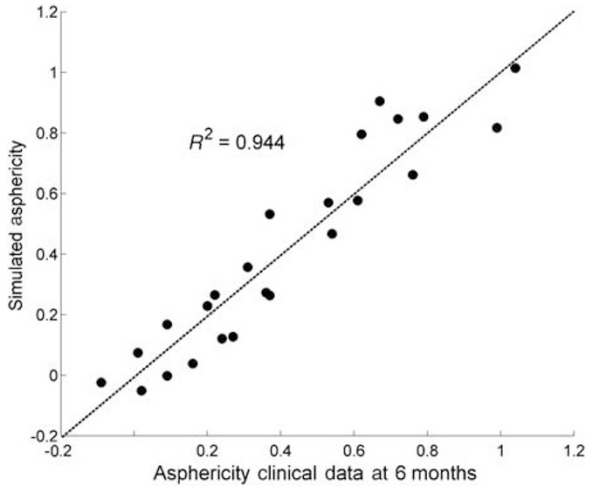

Figure 2 Corneal asphericity after remodelling computed by simulation *vs* Postsurgery (6 months) corneal asphericity reported by Anera *et al*.[22] The computed correlation coefficient is $R^2 = 0.944$.

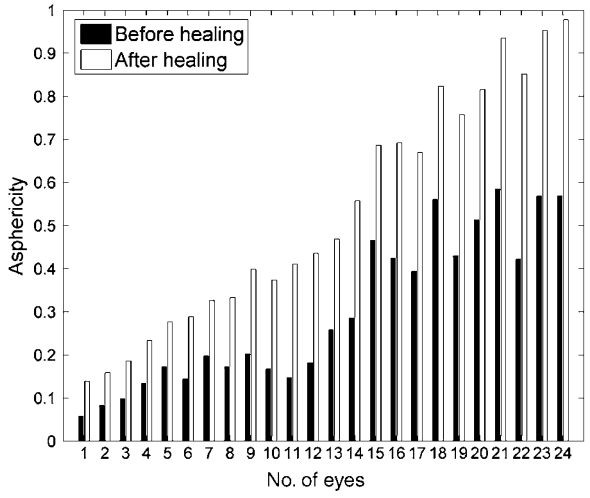

Figure 3 Change in corneal asphericities computed by simulation before and after remodelling. The computational fitting zone size is 4.5 mm. Note that in all eyes, increased postsurgery corneal asphericities.

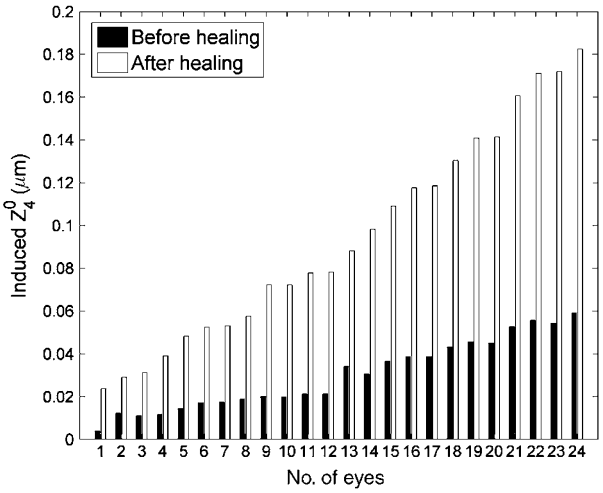

Figure 4 Induced spherical aberration of cornea computed by simulation before and after remodelling. The computational zone size for the spherical aberration is 4.5 mm. Note that in all eyes, a positive spherical aberration is induced.

the exact Munnerlyn formula as the ablation profile. Jimenez *et al*[13] modelled the increase using an ablation profile based on parabolic approximation to the Munnerlyn formula. With that assumption, they found that over 80% of the increase could be attributed to the ablation efficiency reduction caused by the curvature of the cornea. We are able to accurately predict the increased asphericity for individual eyes by two factors: the ablation efficiency reduction caused by corneal curvature and corneal remodelling, which occurs as part of the healing process. Kwon *et al*[16] have shown that in a surgery with a laser having a small Gaussian beam, the corneal asphericity will increase less with the profile based on the Munnerlyn formula than one based on the parabolic approximation, independent of the corneal remodelling process., When we include the corneal remodelling contribution to the postsurgery asphericity values with the profile based on parabolic approximation, we obtain a 30–50% overestimation of the postsurgery asphericities, relative to clinical data.

Contribution to the induced spherical aberration follows the same trend. The remodelling process accounts for 70% of the induced spherical aberration, using an ablation profile based on the Munnerlyn formula. We also expect the induced spherical aberration to increase with the degree of myopia, as shown in Figure 4. The correlation coefficients between the magnitude of the refractive correction and the induced spherical aberration have correlation coefficients of 0.98 and 0.99, respectively, before and after remodelling. The regression equations for induced spherical aberration show that for each dioptre of correction, after remodelling, 0.02 μm of spherical aberration is added to the postsurgery spherical aberration for surgeries performed with a laser having small Gaussian beam.

Our results qualitatively agree with the results reported by Holladay and Janes,[10] Anera *et al*[12] Yoon *et al*,[8] and Marcos *et al*.[23] These trends are observed both clinically and in simulations (see Table 1).

More accurate modelling predictions of postoperative asphericity could be produced if preoperative corneal topography measurements, rather than only asphericities, were available for each eye. Differences between model predictions of corneal asphericity and actual clinical outcomes may be due to ablation

decentration, laser energy or fluence variation, additional biomechanical, or wound healing effects. These factors may degrade the outcomes of custom procedures, which need high precision to minimize eye aberrations and generate the exact desired shape of the cornea.

Conclusions

We have calculated the increase in corneal asphericity and induced spherical aberration after refractive surgery with an ablation profile based on the exact Munnerlyn formula, using a rigorous simulation model. The change in the asphericity is explained by the ablation efficiency reduction in the periphery of cornea (55%) and the remodelling process (45%). The predicted asphericity is in close agreement with the 6-month postoperative clinical measurements, with a correlation coefficient of $R^2 = 0.94$. Simulation results indicate that $\sim$70% of induced spherical aberration is caused by the remodelling process associated with healing. The accurate predictions of the simulation show the validity of the model and may allow for the use of the model to design customized ablation profiles to reduce induced aberrations.

Acknowledgements

We thank Proffessor José Ramón Jiménez for providing the clinical data and helpful discussions. This study was supported by Alcon.

References

1 Miller JM, Anwaruddin R, Straub J, Schwiegerling J. Higher order aberrations in normal, dilated, intraocular lens, and laser *in situ* keratomileusis corneas. *J Refrac Surg* 2002; **18**: S579–S583.
2 Mrochen M, Kaemmerer M, Mierdel P, Seiler T. Increased higher-order optical aberrations after laser refractive surgery: a problem of subclinical decentration. *J Cataract Refract Surg* 2001; **27**: 362–369.
3 Moreno-Barriuso E, Lloves JM, Marcos S, Navarro R, Llorente L, Barbero S. Ocular aberrations before and after myopic corneal refractive surgery: LASIK-induced changes measured with laser ray tracing. *Invest Ophthalmol Vis Sci* 2001; **42**: 1396–1403.
4 Oshika T, Klyce SD, Applegate RA, Howland HC, Danasoury MAE. Comparison of corneal wavefront aberrations after photorefractive keratectomy and laser *in situ* keratomileusis. *Am J Ophthalmol* 1999; **127**: 1–7.
5 Schwiegerling J, Snyder RW. Corneal ablation patterns to correct for spherical aberration in photorefractive keratectomy. *J Cataract Refract Surg* 2000; **26**: 214–221.
6 Marcos S, Cano D, Barbero S. Increase in corneal asphericity after standard laser *in situ* keratomileusis for myopia is not inherent to the munnerlyn algorithm. *J Refract Surg* 2003; **19**: S592–S596.
7 Hersh PS, Fry K, Blaker JW. Spherical aberration after laser *in situ* keratomileusis and photorefractive keratectomy clinical results and theoretical models of etiology. *J Cataract Refract Surg* 2003; **29**: 2096–2104.
8 Yoon G, MacRae S, Williams DR, Cox IG. Causes of spherical aberration induced by laser refractive surgery. *J Cataract Refract Surg* 2005; **31**: 127–135.
9 Holladay JT, Dudeja DR, Chang J. Functional vision and corneal changes after laser *in situ* keratomileusis determined by contrast sensitivity, glare testing, and corneal topography. *J Cataract Refract Surg* 1999; **25**: 663–669.
10 Holladay JT, Janes JA. Topographic changes in corneal asphericity and effective optical zone after laser *in situ* keratomileusis. *J Cataract Refract Surg* 2002; **28**: 942–947.
11 Mrochen M, Seiler T. Influence of corneal curvature on calculation of ablation patterns used in photorefractive laser surgery. *J Refract Surg* 2001; **17**: S584–S587.
12 Anera RG, Jiménez JR, Barco LJD, Hita E. Changes in corneal asphericity after laser refractive surgery, including reflection losses and nonnormal incidence upon the anterior cornea. *Optics Letters* 2003; **28**: 417–419.
13 Jiménez JR, Anera RG, Barco LJd. Equation for corneal asphericity after corneal refractive surgery. *J Refract Surg* 2003; **19**: 65–69.
14 Gatinel D, Hoang-Xuan T, Azar DT. Determination of corneal asphericity after myopia surgery with the excimer laser: a mathematical model. *Invest Ophthalmol Vis Sci* 2001; **42**: 1736–1742.
15 Dorronsoro C, Cano D, Merayo-Lloves J, Marcos S. Experiments on PMMA models to predict the impact of corneal refractive surgery on corneal shape. *Optics Express* 2006; **14**: 6142–6156.
16 Kwon Y, Choi M, Bott S. Impact of ablation efficiency reduction on postsurgery corneal asphericity: simulation of the laser refractive surgery with a flying spot laser beam. *Optics Express* 2008; **16**: 11808–11821.
17 Huang D, Tang M, Shekhar R. Mathematical model of corneal surface smoothing after laser refractive surgery. *Am J Ophthal* 2003; **135**: 267–278.
18 Kwon Y. Surgery simulation—computer modeling of ablation crater profiles and corneal curvature map. *Alcon Lab* 2007; technical report 2017–2029.
19 Jimenez JR, Anera RG, Barco LJd, Hita E. Effect on laser-ablation algorithms of reflection losses and nonnormal incidence on the anterior cornea. *Appl Phys Lett* 2002; **81**: 1521–1523.
20 Munnerlyn CR, Koons SJ, Marshall J. Photorefractive keratectomy: a technique for laser refractive surgery. *J Cataract Refract Surg* 1988; **14**: 46–52.
21 Deutsch TF, Geis MW. Self-developing UV photoresist using excimer laser exposure. *J Appl Phys* 1983; **54**: 7201–7204.
22 Anera RG, Jimenez JR, Barco LJd, Bermudez J, Hita E. Changes in corneal asphericity after laser *in situ* keratomileusis. *J Cataract Refract Surg* 2003; **29**: 762–768.
23 Marcos S. Spherical aberration: biomechanics or physical laser effects? Preseneted in *Wavefront Congress* 2006 Meeting (Nassau, Bahamas, 6 January 2006).